International Journal of Thermophysics, Vol. 24, No. 3, May 2003 (© 2003)

Simultaneous Measurement of Thermophysical Properties and Dielectric Properties of PZT-Based Ferroelectric Ceramics by Thermal Radiation Calorimetry[1]

K. Morimoto,[2] A. Uematsu,[2] S. Sawai,[2] K. Hisano,[2,3] and T. Yamamoto[4]

Simultaneous measurements of thermophysical properties and dielectric properties have been performed for PZT-based ferroelectric ceramics. An apparatus based on thermal radiation calorimetry was used in the present measurements. Anomalies in the thermophysical properties were observed near the ferroelectric-to-paraelectric phase transition temperature. The anomalous peak was at almost the same temperature as the inflection point of the dielectric constant. It was found that modification of PZT with increasing Nb, Mg, Zn, and Sr causes a decrease of the Curie temperature and an increase of the hysteresis phenomena for the phase transition, and the values of the thermal conductivity increase with temperature similar to amorphous materials.

KEY WORDS: dielectric constant; phase transition; PZT; simultaneous measurement; specific heat capacity; thermal conductivity; thermal diffusivity; thermal radiation calorimetry.

1. INTRODUCTION

PZT ($Pb(Zr_x, Ti_{1-x})O_3$) is well known as a ferroelectric material, with high piezoelectric and dielectric characteristics. It has been demonstrated that

[1] Paper presented at the Sixteenth European Conference on Thermophysical Properties, September 1–4, 2002, London, United Kingdom.

[2] Department of Applied Physics, National Defense Academy, Hashirimizu 1-10-20, Yokosuka 239-8686, Japan.

[3] To whom correspondence should be addressed. E-mail: hisano@nda.ac.jp

[4] Department of Communications Engineering, National Defense Academy, Hashirimizu 1-10-20, Yokosuka 239-8686, Japan.

0195-928X/03/0500-0821/0 © 2003 Plenum Publishing Corporation

the PZT piezoelectric characteristics can be improved with the use of additives. Okazaki [1] reported the properties of PZT modified with Nb, Mn, and La, while Kanai et al. [2] observed an improvement in the dielectric constant for PZT doped with Ca, Sr, and Ba. Rimoldi et al. [3] observed larger values of remnant polarization and a smaller coercive field for PZT modified with Nb. The relaxor ferroelectrics PMN ($Pb(Mg_{1/3}Nb_{2/3})O_3$) and PZN ($Pb(Zn_{1/3}Nb_{2/3})O_3$) are characterized by a diffuse maximum of dielectric constant of extremely high value associated with significant frequency dispersion. These relaxors form solid solutions with PT ($PbTiO_3$) and PZ ($PbZrO_3$). Gupta and Viehland [4] reported that a relatively small concentration of PMN has significant influences on the maximum constant of the dielectric properties and the Curie temperature. Several papers have reported results for properties, for example, dielectric and structural properties, of PMN-PT [5], PZN-PT [6], and PMN-PT-PZ [7]. On the other hand, when if it is used as a capacitor for an electrical circuit, the values of thermophysical properties are essential for it. However, as far as we are aware, there has been little published information relating to the thermophysical properties.

Thermal radiation calorimetry (TRAC) makes it possible to measure the thermophysical and dielectric properties simultaneously [8, 9]. The measurement is performed in a vacuum chamber in which a disk-shaped specimen is heated and cooled slowly by thermal radiation from double flat heaters [10]. The specific heat capacity can be obtained directly from the temperatures of the specimen and heater, and the time rate of the specimen temperature change. This calorimetry can also be used to perform simultaneous measurements of specific heat capacity, thermal conductivity, and thermal diffusivity [11]. A flat heater is used to irradiate the specimen on one face in order to impose a temperature gradient within the specimen for the measurement of three thermophysical properties. Because three quantities are obtained independently, a self-check of the reliability of the results is made. The method of measurement is based on the quasi-steady state approximation that the spatial temperature distribution is assumed to be parabolic in the direction of specimen thickness in a one-dimensional system when the specimen temperature is changed slowly [11].

In the present work, simultaneous measurements of the thermophysical and dielectric properties are performed for three types of commercial PZT-based ferroelectric ceramics. The temperature ranges are from 440 to 700 K for the simultaneous measurement of the specific heat capacity and dielectric properties, and from 500 to 750 K for the simultaneous measurement of the three thermophysical properties.

2. EXPERIMENT

2.1. Simultaneous Measurement of Specific Heat Capacity and Dielectric Properties

A theory of the measurement technique has already been presented in detail in previous papers [8–10]. The heat power exchange between a disk-shaped specimen and flat heaters in a vacuum chamber by thermal radiation is shown schematically in Fig. 1. When a disk-shaped specimen (mass M, surface area A, specific heat capacity C_p) is heated and cooled on both surfaces only by thermal radiation from the heaters in a vacuum chamber, the time rate of the specimen temperature change is described by

$$MC_p \frac{dT_s}{dt} = E_h A(I_h - I_s) - E_s A(I_s - I_r) - \frac{dQ_s}{dt} \tag{1}$$

where I is the emissive power per unit area of blackbody radiation, which is equal to σT^4 (σ is the Stefan–Boltzmann constant and T is the temperature). Subscripts s, h, and r refer, respectively, to the specimen, the heater, and the wall of the vacuum chamber, which is kept at a certain temperature.

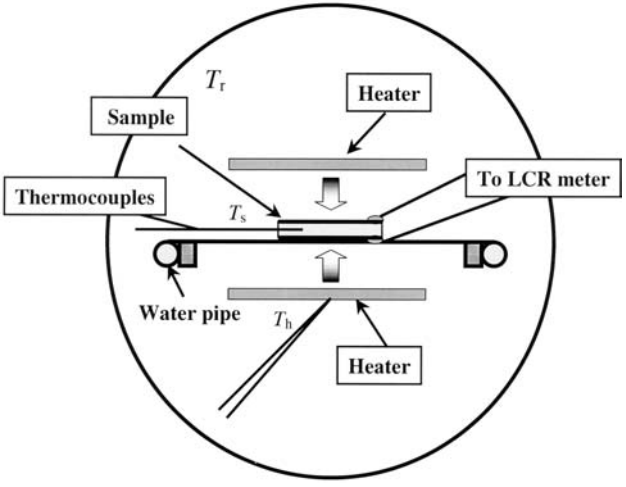

Fig. 1. Schematic setup for the simultaneous measurement of specific heat capacity and dielectric constant.

dQ_s/dt is the conductive heat loss per unit time through thermocouple leads, the leads for measurement of the electric quantity, and specimen supports. E_h and E_s are the *effective emissivities* arising from the radiant heat transfer between the specimen, the heater, and the chamber wall.

The specific heat capacity C_p is derived from Eq. (1) at the same specimen temperature T_s for the heating and cooling processes:

$$\frac{C_p}{E_h} = \frac{A(I_h - I'_h)}{M\left(\frac{dT_s}{dt} - \frac{dT'_s}{dt}\right)} \tag{2}$$

where (′) indicates the cooling process. $dQ_s/dt \cong dQ'_s/dt$ is assumed to be at the same T_s. C_p can be estimated if E_h is evaluated experimentally by use of a specimen whose specific heat is accurately known at various temperatures. When thermal hysteresis in the phase transition is observed between the heating and cooling processes, C_p is obtained by

$$\frac{C_p}{E_h} = \frac{A(I_h - I_{h0})}{M\frac{dT_s}{dt}} \tag{3}$$

where I_{h0} is that at steady state and satisfies the following relation;

$$E_h A(I_{h0} - I_s) - E_s A(I_s - I_r) - \frac{dQ_{s0}}{dt} = 0 \tag{4}$$

Outside the phase transition region, where $C_p = C'_p$, I_{h0} can be calculated by the following equation,

$$I_{h0} = I_h - \frac{MC_p}{AE_h}\frac{dT_s}{dt} = I_h - \frac{I_h - I'_h}{\frac{dT_s}{dt} - \frac{dT'_s}{dt}}\frac{dT_s}{dt} \tag{5}$$

The values of I_{h0} in the phase transition region are estimated by interpolation with a proper function.

As shown in the schematic in Fig. 1, a disk-shaped specimen 32 mm in diameter and 3.0 mm thick, and two flat 50×60 mm alumina ceramic heaters are set in a water-cooled vacuum chamber, which can be evacuated to 10^{-3} Pa during the measurement. The specimen is placed in the center of two heaters. An alumel-chromel thermocouple sheathed in a tube of Inconel 600 (Rikou Seiki, Tokyo, Japan), 0.5 mm in diameter, is inserted into a hole drilled in the side to measure the specimen temperature. The

temperature of the heater is measured with an alumel-chromel thermocouple (0.1 mm in diameter), attached to the heater. Copper is evaporated on both surfaces of the specimen as electrodes and a copper wire (0.1 mm in diameter) attached on each side to measure the dielectric properties. Measurements of capacitance, as a function of temperature, are performed with a LCR meter (Hewlett Packard 4284A) operating at a frequency of 100 kHz. The surfaces of the specimens, the heater, and the inside wall of the chamber are coated with colloidal graphite (Acheson, Electrodag188) for blackening their surfaces. The heater current was controlled so that the ramp rate of the specimen temperature becomes about 4 $K \cdot min^{-1}$. Copper was used as a reference material to obtain the value of E_h. The relative error involved in the obtained values is $\pm 3\%$ for the specific heat capacity.

In the study, three types of commercial PZT ceramics (Hizirco L (specimen #1), MPT (#2), AL (#3), Hayashi Chemical Indust. Co. Ltd., Japan) were prepared. These are used for the piezoelectric buzzer, the piezoelectric transformer, and the actuator, respectively. The composition was analyzed by X-ray fluorescence analysis and inductively coupled plasma spectrometry. The results are shown in Table I. The existence of a small element (< 2 mol%) could have not been identified correctly in the present investigation. Specimens #1, #2, and #3 are assumed to be PZT modified with a small amount of Nb, $Pb((Zn_{1/3}, Nb_{2/3})(Zr, Ti))O_3$, and $(Pb, Sr)((Zn_{1/3}, Nb_{2/3}), (Mg_{1/3}, Nb_{2/3}), (Zr, Ti))O_3$, respectively.

2.2. Simultaneous Measurement of Three Thermophysical Properties

The theory of the simultaneous measurement technique of three thermophysical properties has already been presented in detail [11]. As shown in the schematic in Fig. 2, it is based on a one-dimensional system in

Table I. Composition of Three Types of Commercial PZT Ceramic Specimens, (Analyzed by X-ray Fluorescence Analysis and Inductively Coupled Plasma Spectrometry; Mol-Ratio of Ti, Zr, Nb, and other Elements to Pb for the Case when mol% of Pb is 100)

	Specimen #1	Specimen #2	Specimen #3
Pb	100	100	100
Ti	45–46	40–42	39–41
Zr	49–52	38–45	33
Nb	~ 1	12–14	19–21
Zn		~ 5	< 5
Mg			~ 10
Sr			< 5

which a disk-shaped specimen (specific heat capacity C_p, thermal conductivity λ, thermal diffusivity a, density ρ, thickness L) is heated and cooled on one face by thermal radiation in a vacuum chamber, and exchanges its temperature in time t and in space x. In this system, the diffusion equation and the Weierstrass approximation theorem are required to describe the heat diffusion.

$$\frac{\partial T(x,t)}{\partial t} = a\frac{\partial^2 T(x,t)}{\partial x^2} \tag{6}$$

$$T(x,t) = \sum_{n=0}^{\infty} \alpha_n(t)\frac{x^n}{n!} \tag{7}$$

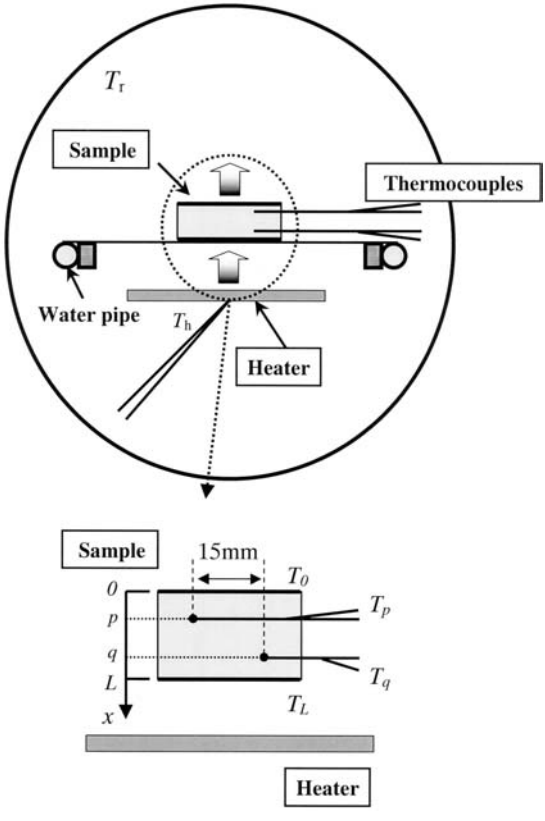

Fig. 2. Schematic setup for the simultaneous measurement of three thermophysical properties.

where $T(x,t)$ is the temperature distribution within the specimen. The above two equations combine to give the general solution:

$$T(x, t) = \sum_{n=0}^{\infty} \left\{ \sum_{m=0}^{\infty} \frac{(at)^m}{m!} \alpha_{n+2m}(t) \right\} \frac{x^n}{n!} \tag{8}$$

The energy exchange at the back specimen surface ($x = 0$), facing the chamber wall maintained at room temperature, is written as

$$\lambda \left(\frac{\partial T}{\partial x} \right)_{x=0} A = \varepsilon (I_0 - I_r) A \tag{9}$$

where ε and A are the surface emissivity and the specimen surface area, respectively. I_0 is the radiation power per unit area and time emitted from the back surface. For the case of $n = 2$, $T(x, t)$ is derived from Eqs. (6) and (7);

$$T(x, t) = a\alpha_2 t + \alpha_1 x + \tfrac{1}{2} \alpha_2 x^2 + \alpha_0(0) \tag{10}$$

where $\alpha_1(t)$ is constant and $\alpha_2(t)$ is zero in steady state, and both $\alpha_1(t)$ and $\alpha_2(t)$ are constant in quasi-steady state. For the case of $n = 3$, $T(x, t)$ is derived from Eqs. (6) and (7);

$$T(x, t) = \{a\alpha_2 t + \alpha_0(0)\} + \{a\alpha_3 t + \alpha_1(0)\}\, x + \tfrac{1}{2} \alpha_2 x^2 + \tfrac{1}{6} \alpha_3 x^3 \tag{11}$$

where both $\alpha_2(t)$ and $\alpha_3(t)$ are constant in quasi-steady state. If the following condition,

$$\frac{\left(\frac{\partial T}{\partial t} \right)_{x=L} - \left(\frac{\partial T}{\partial t} \right)_{x=0}}{\left(\frac{\partial T}{\partial t} \right)_{x=0}} \ll 1 \tag{12}$$

is valid, the following equation is derived from the above equations:

$$\lambda \frac{T_L - T_0}{L} = \varepsilon (I_0 - I_r) + \frac{1}{2} C_p \rho L \frac{dT}{dt} \tag{13}$$

Subscript L refers to the front surface facing the heater. Considering both heating and cooling processes of the system, the above equation can be used to derive the following equations at the same back surface

temperature ($T_0 = T'_0$) if the temperature change rate of the specimen is the same:

$$\lambda = \frac{2L}{T_L + T'_L - 2T_0} \varepsilon (I_0 - I_r) \tag{14}$$

$$a = \frac{\lambda}{C_p \rho} = \frac{L^2}{2(T_L - T'_L)} \left(\frac{dT}{dt} - \frac{dT'}{dt} \right) \tag{15}$$

where (′) indicates the cooling process. At the same front surface temperature ($T_L = T'_L$), C_p is given by

$$C_p = \frac{E_h (I_h - I'_h) - \varepsilon (I_0 - I'_0)}{\rho L (dT/dt - dT'/dt)} \tag{16}$$

As shown in the schematic in Fig. 2, a specimen 32 mm in diameter and 5.0 mm thick and a flat heater are set in the water-cooled vacuum chamber with a specimen above the center of the heater. The temperature gradient within the specimen is measured by use of two sheathed alumel-chromel thermocouples set in the holes drilled in the side. The temperature of the heater is measured by an alumel-chromel thermocouple, which was attached to the heater. The heater current is controlled so that dT/dt is kept around 5 $K \cdot min^{-1}$ in both the heating and cooling processes. The surfaces of the specimens, the heater, and the inside wall of the chamber were also coated with colloidal graphite. The specimen surfaces were plated with silver metal before blackening. Copper was also used as a reference material to obtain the value of E_h. The relative errors involved in the obtained values are $\pm 5\%$, $\pm 5\%$, and $\pm 10\%$ for the specific heat capacity, the thermal conductivity, and the thermal diffusivity, respectively.

For this experiment, two commercial PZT ceramic specimens (specimens #1 and #2) were prepared. The thermocouple hole positions of p and q in the direction x are, respectively, 0.80 ± 0.01 and 4.25 ± 0.01 mm for the specimen #1, and 0.85 ± 0.01 and 4.28 ± 0.01 mm for the specimen #2. The thermocouple separation was about 15 mm at the side surface.

3. RESULTS AND DISCUSSION

Figures 3 to 5 show the results of the simultaneous measurements of C_p, ε_s, and tan δ of specimens #1, #2, and #3, respectively. The filled and open circle data points refer to the heating and cooling processes, respectively. Anomalies in C_p associated with the ferroelectric-to-paraelectric phase transition are observed for all specimens as well as abrupt changes in ε_s and tan δ. The Curie temperatures of the specimens decrease in the order

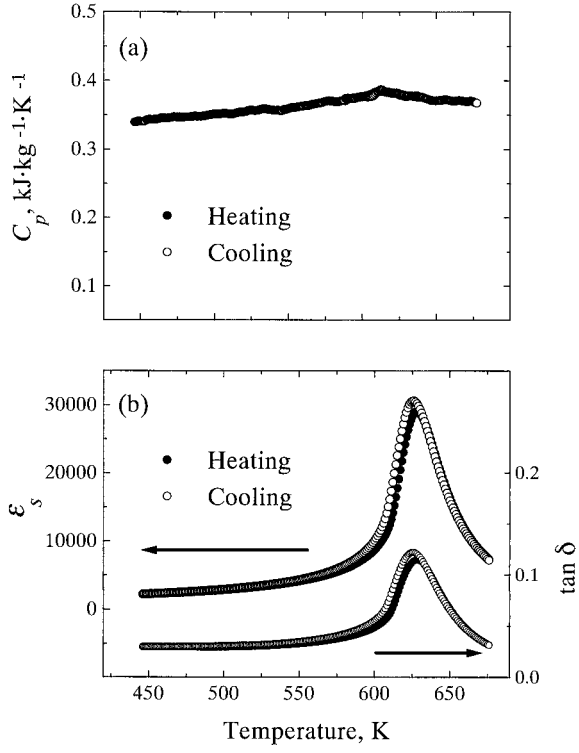

Fig. 3. Temperature dependence of (a) C_p, (b) ε and tan δ for specimen #1. The filled and open circle data points refer to the heating and cooling processes, respectively.

of #1, #2, and #3. The temperature at which the anomalous peak of C_p, the maxima of ε_s and $d\varepsilon_s/dT$ appear, are listed in Table II. The anomalous peak of C_p is observed at a lower temperature than that of the maximum of ε_s, but almost at the same temperature as the inflection point of ε_s for all specimens. The same results have been reported for $Ba_xSr_{1-x}TiO_3$ ceramics by the authors of this study [9].

For specimen #1, the excess specific heat due to the phase transition is observed over a wide temperature range. The temperature range becomes narrow in the order of #1, #2, and #3. Hysteresises of C_p, ε_s, and tan δ around the Curie point are observed clearly for specimen #2 and #3 with that for specimen #3 much larger than that for #2. Slightly different paths of ε are observed for specimen #1 for the heating and cooling processes, but hysteresis of C_p was not detected and the peak around the Curie temperature was broad. The anomaly in C_p for specimen #1 is considered to be

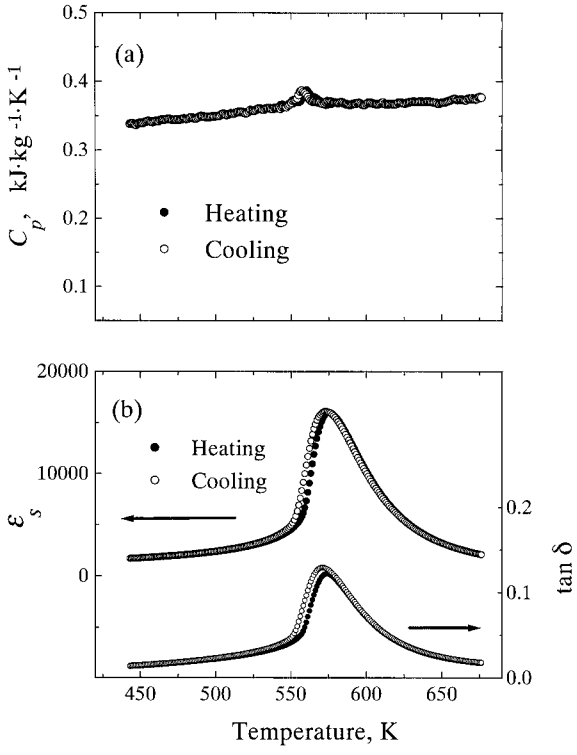

Fig. 4. Temperature dependence of (a) C_p, (b) ε and tan δ for specimen #2. The filled and open circle data points refer to the heating and cooling processes, respectively.

second-order. The second-order-type anomaly, which extends over a wide temperature range such as that of #1, was reported for hexagonal barium titanate [12]. Dai et al. [13] reported that the phase transition of PZT with Zr/Ti ratios from 80/20 to 60/40, and probably to 55/45, is second-order although that of PZT 95/5 is first-order. They observed the maximum peak of ε_s at about 640 K for PZT when the Zr/Ti ratio is 55/45, and for Nb-doped $Pb(Zr_{0.45}Ti_{0.55})O_3$. Paiva-Santos et al. [14] reported that the Curie temperature decreased and the maximum dielectric constant increased with increasing Nb concentration up to 10 mol%. The present results for specimen #1 agree with their results, however, the maximum value of ε is very high. It is unknown whether the small amount of Nb and the other elements influence strongly the maximum value of ε_s to this extent. For specimens #2 and #3, the Curie temperatures are lower than that of a pure PZT. Thermal hysteresises of C_p are observed and

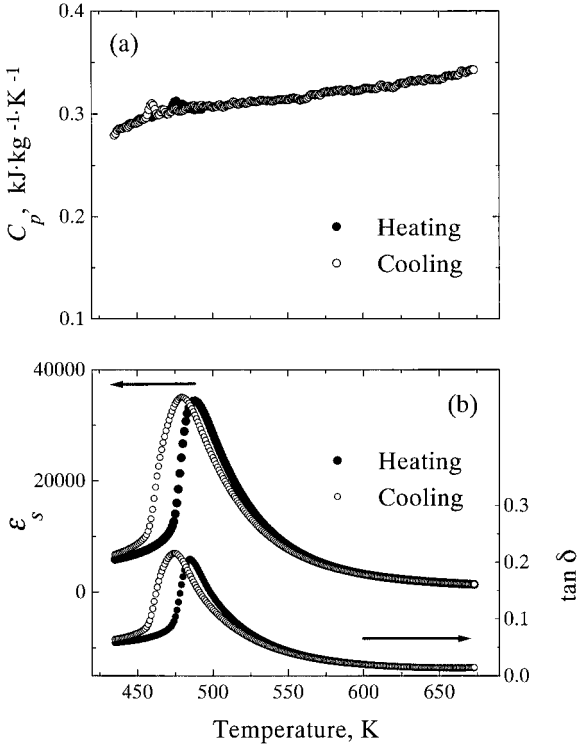

Fig. 5. Temperature dependence of (a) C_p, (b) ε and tan δ for specimen #3. The filled and open circle data points refer to the heating and cooling processes, respectively.

excesses of the specific heat appear in a narrower range than that of specimen #1. These phase transition types are first-order, which is different from that of specimen #1. These results indicate that modifications with Nb, Mg, Zn, and Sr, or the formation of the solid solution with PMN and/or PZN, cause the decrease of the Curie temperature and the change of the phase transition type from second-order to first-order.

Figures 6 and 7 show the results of simultaneous measurements of C_p, λ, and a of specimens #1 and #2, respectively. Open circle data points shown in Figs. 6a and 7a indicate the results calculated from λ and a shown in Figs. 6b and 7b. Anomalies in C_p and a are also found around the phase transition temperature. The temperature at which the anomalous peak of C_p and a appear are listed in Table III. Anomalous peaks of C_p and a are also observed at almost the same temperature as the inflection point of ε_s.

Table II. Temperatures of Anomalous Peaks of C_p and Maxima of ε_s and $d\varepsilon_s/dT$

	C_p		Maximum of ε		Maximum of $d\varepsilon/dT$	
	Heating	Cooling	Heating	Cooling	Heating	Cooling
Specimen #1	613	613	628	626	615	613
Specimen #2	560	557	575	572	562	559
Specimen #3	476	460	488	480	477	461

As far as the specific heat capacity C_p is concerned, the result for specimen #1 in Fig. 6a is almost consistent with those in Fig. 3a. However, the anomaly for specimen #2 in Fig. 7a is wider than that in Fig. 4a. Figure 8 shows the temperature difference between the surfaces of specimen #2 for both processes. The filled and open circle data points refer to the heating

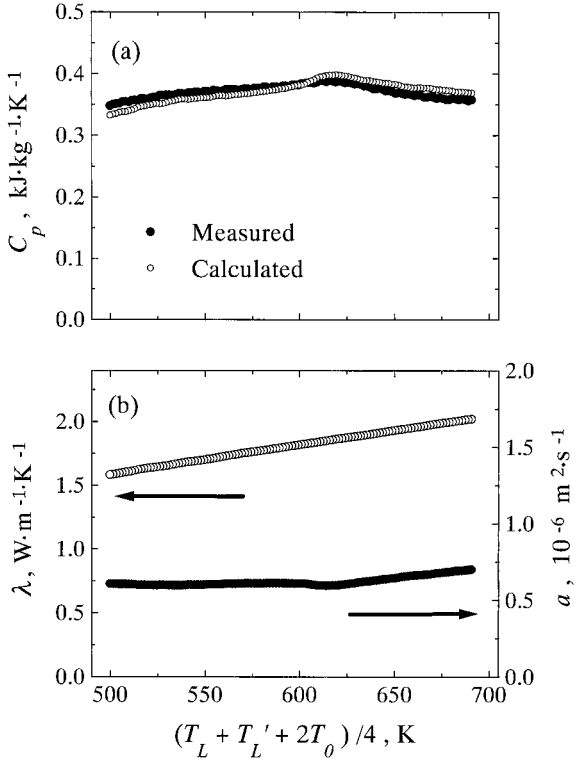

Fig. 6. Temperature dependence of (a) C_p, (b) λ and a for specimen #1. Open circle data points in (a) show the results calculated from λ and a shown in (b).

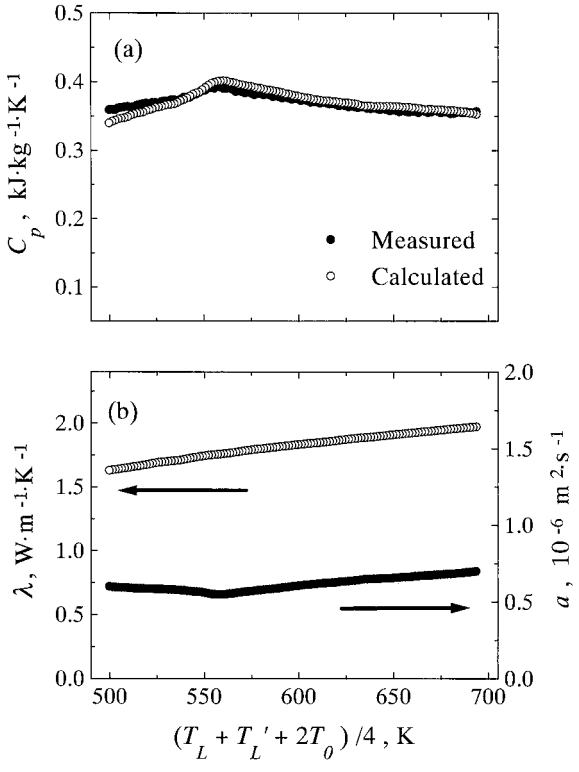

Fig. 7. Temperature dependence of (a) C_p, (b) λ and a for specimen #2. Open circle data points in 7 (a) show the results calculated from λ and a shown in (b).

and cooling processes, respectively. As shown in Fig. 8, the difference of both surface temperatures is about 15 K at the phase transition temperature. This result may cause the broad width in the anomalies.

In general, the values of λ of amorphous materials such as glasses increase with temperature and those of crystallized materials decrease.

Table III. Temperatures of Anomalous Peaks of C_p and a

	C_p		
	Measured	Calculated	a
Specimen #1	616	617	617
Specimen #2	557	559	559

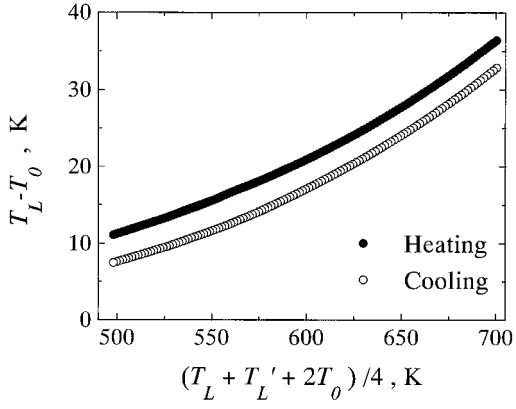

Fig. 8. Temperature difference between the specimen surfaces of specimen #2. The filled and open circle data points refer to the heating and cooling processes, respectively.

From the results in Figs. 6b and 7b, it seems that these ceramics show behaviors similar to amorphous materials.

4. CONCLUSION

Simultaneous measurements of thermophysical properties and dielectric properties have been performed for three types of commercial PZT-based ferroelectric ceramics with an apparatus based on thermal radiation calorimetry. Anomalies in C_p and a are observed near the ferroelectric-to-paraelectric phase transition temperature. Anomalous peak is at almost the same temperature as the inflection point of ε_s. Modification of PZT with increasing Nb, Mg, Zn, and Sr causes a decrease of the Curie temperature and an increase of the hysteresis phenomena at the phase transition, and a change of the phase transition type from second-order to first-order. The values of λ increase with temperature, similar to amorphous materials.

REFERENCES

1. K. Okazaki, *Ferroelectrics* **25**:337 (1993).
2. H. Kanai, O. Furukawa, H. Abe, and Y. Yamashita, *J. Am. Ceram. Soc* **77**:2620 (1994).
3. L. C. Rimoldi, M. A. Zaghete, J. A. Varela, M. Cilense, and C. O. Paiva-Santos. *Ceramica* **42**:483 (1996).
4. S. M. Gupta and D. Viehland, *J. Appl. Phys.* **83**:407 (1998).
5. S. W. Choi, T. R. Shrout, S. J. Jang, and A. Bhalla, *Ferroelectrics* **100**:29 (1989).
6. J. Kuwata, K. Uchino, and S. Nomura, *Ferroelectrics* **37**:579 (1981).

7. H. Ouchi, K. Nagano, and S. Hasegawa, *J. Am. Ceram. Soc.* **169**:309 (1995).
8. K. Morimoto, S. Sawai, K. Hisano, and T. Yamamoto, *Ferroelectrics* **227**:133 (1999).
9. S. Sawai, H. Tanaka, K. Morimoto, K. Hisano, and T. Yamamoto, *Ferroelectrics* **242**:59 (2000).
10. K. Morimoro, S. Sawai, and K. Hisano, *Int. J. Thermophys.* **20**:709 (1999).
11. K. Hisano, S. Sawai, and K. Morimoro, *Int. J. Thermophys.* **20**:733 (1999).
12. Y. Akishige, T. Atake, Y. Saito, and E. Sawaguchi, *J. Phys. Soc. Jpn.* **57**:718 (1988).
13. X. Dai, Z. Xuand, and D. Viehland, *J. Am. Ceram. Soc.* **78**:2815 (1995).
14. C. O. Paiva-Santos, C. F. Oliveira, W. C. Las, M. A. Zaghete, and J. A. Varela, *Mater. Res. Bull.* **35**:15 (2000).